RADIATIVE CORRECTIONS IN BOUND STATES*

Robert Szafron

Physik Department T31, Technische Universität München
James Franck Straße 1, 85748 Garching, Germany

(Received November 6, 2017)

We give a brief overview of the recent progress in the computation of QED radiative corrections for various processes involving bound states. Precision measurements of bound state properties, such as the Lamb shift of hydrogen atom and g-factor of a bound electron, and searches for rare transitions, such as $B_s \to \mu^+\mu^-$ or muon–electron coherent conversion, allow for a precise tests of the Standard Model. A comparison between the theory and the experiment cannot be done without the knowledge of the higher order effects, which sometimes receive unexpected enhancement factors.

DOI:10.5506/APhysPolB.48.2183

1. Introduction

Various bound states involving electrons, muons, and quarks offer opportunities to test the Standard Model (SM) and can lead to a discovery of new physics signal [1]. Working with the bound states comes at a cost of more complicated theoretical description than the one used for typical scattering experiments. The bound states introduce new, dynamically generated scales; *e.g.* in hydrogen atom, the momentum αm_e and energy $\alpha^2 m_e$ of the electron are dynamically generated. In addition, the usual perturbative approach based on Feynman diagrams breaks down. Typically, a certain class of diagrams has to be resummed to obtain the leading order prediction; *e.g.* so-called ladder diagrams need to be resummed in hydrogen atom to obtain the leading Lamb shift at $\mathcal{O}(\alpha(Z\alpha)^4)$.

Modern effective field theory (EFT) methods offer simplifications that allow computing bound state properties in a systematic way. Once the scales that appear in a given problem are separated, the EFT is constructed such that only operators with a well-defined power-counting appear.

* Presented at the XLI International Conference of Theoretical Physics "Matter to the Deepest", Podlesice, Poland, September 3–8, 2017.

In this proceedings, we are going to give some examples of the recent computations of the QED corrections in QED and QCD bound states. Typically, these corrections reveal unexpected enhancement factors and their effect is larger than it is estimated by naive power-counting. We shall consider two cases of observables. The static ones are those related to asymptotic properties of the bound state like, for example, energy levels of a hydrogen atom. On the other hand, when the bound particles decay, then dynamical observables appear, for example, decay width of the system or spectrum of daughter particles.

2. Static observables

First, we focus on the static observables, such as energy levels of the hydrogen or the gyromagnetic factor of the bound electron. Computation of the radiative corrections to the energy levels of the hydrogen spectrum has a long history, starting from the famous computation of Bethe [2]. The self-energy corrections to the energy of the ground state of a hydrogen atom can be represented as a double series in $\frac{\alpha}{\pi}$ that is related to the number of photon loops and in $Z\alpha$ that parametrizes binding corrections. Some terms in the expansion are additionally enhanced by logarithms of $Z\alpha$

$$\begin{aligned}\frac{\Delta E}{m_e} &= \frac{\alpha}{\pi}(Z\alpha)^4\left(A_{41}\ln(Z\alpha)^{-2} + A_{40} + Z\alpha A_{50} + \ldots\right)\\ &\quad + \left(\frac{\alpha}{\pi}\right)^2(Z\alpha)^4\left(B_{40} + Z\alpha B_{50} + (Z\alpha)^2 B_{63}\ln^3(Z\alpha)^{-2} + \ldots\right). \quad (1)\end{aligned}$$

For the most recent values of the known coefficients, see CODATA [3]. Logarithmic enhancement appears when an ultra-soft photon with momentum $k \sim m_e Z\alpha$ is exchanged or when the matrix element of an effective operator is divergent.

Coefficient B_{61} has been computed in [4, 5]. However, the so-called light-by-light (LBL) contributions (see Fig. 1) were not included in these works. It turns out that LBL diagrams contribute to the matching on some of the $\frac{1}{m_e^3}$ operators of the non-relativistic QED

$$\mathcal{L}_{\text{NRQED}} \supset \psi^\dagger\left(c_A\frac{\left(\vec{B}^2 - \vec{E}^2\right)}{m_e^3} - c_B\frac{\vec{E}^2}{m_e^3} + c_s\frac{\left(\vec{\sigma}\cdot\vec{B}\right)\left(\vec{\nabla}\cdot\vec{E}\right)}{m_e^3}\right)\psi\,. \quad (2)$$

The first two operators contribute to the B_{61} coefficient because the expectation value of the electric field squared $\vec{E}^2 \sim \frac{1}{r^4}$ is divergent in S-states of the hydrogen. This is an example of a logarithmic contribution not induced by the ultra-soft photons. The LBL corrections computed in [6] decrease the $1S$–$2S$ energy splitting in hydrogen by 280 Hz, a value much larger than the experimental precision [7].

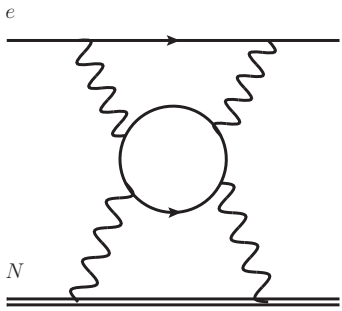

Fig. 1. An example diagram with light-by-light contribution to the Lamb shift. The leading contribution is $\alpha^2(Z\alpha)^5$ and the subleading term $\alpha^2(Z\alpha)^6$ is logarithmically enhanced.

The last operator in Eq. (2) is spin-dependent. It affects the bound electron g-factor at the order of $\alpha^2(Z\alpha)^4$, as predicted by the velocity power-counting rules. The correction affects the electron mass determination [8, 9] and comparison between the theory and the experiment. It is also important because of the recent improvements in the theory of the bound g-factor [10–12] that greatly reduce the theoretical error. This new results facilitate tests of the SM and improvement in determination of fundamental constants, such as atomic electron mass and α. At present, the free electron $g-2$ is used to determine α, but in the future, the bound electron g-factor may serve as a new, more precise source of α [13]. This will allow to use accurate electron $g-2$ experiments to test the theory [14] and thus provide a check of the persisting muon $g-2$ anomaly [15–18].

The EFT methods can be also used to construct new observables that can disentangle short- and long-distance physics [19] and shed some light on the so-called proton radius problem [20]. In the light of the anticipated progress of the experiments, the careful checks and improvements in the theory of the hydrogen spectrum must be performed.

3. Dynamical observables

A spectrum and decay rate of a bound particle are typical examples of dynamical observables. The binding potential may be of the QED origin, like in the case of muonium or muonic atoms; or in the case of mesons, the QCD may be responsible for the binding.

3.1. Decay of muonic atoms

For the bound muon, the spectrum needs to be accurately predicted to match the precision of upcoming experiments that will search for muon–

electron conversion [21, 22]. Observation of the conversion will be a clear signal of new physics. The dominant SM background in conversion searches is the so-called muon decay in orbit (DIO). The leading QED radiative corrections to the DIO spectrum have to be evaluated numerically [23] and using effective field theory methods [24–26]. The dominant corrections are enhanced by the large collinear logarithm of the ratio of the muon mass m_μ to the electron mass m_e. The bound state physics generates dynamically also logarithms of $Z\alpha$ that can be explained as running of the electromagnetic coupling constant α up to the non-perturbatively generated scale $m_\mu Z\alpha$.

The corrections to the muon–electron conversion are also important because they reduce the number of electrons expected within the experimental signal window by several percent. Radiation of real photons reduces the electron energy and modifies the leading order conversion spectrum

$$\frac{m_\mu}{\Gamma_0}\frac{\mathrm{d}\Gamma}{\mathrm{d}E_e} = m_\mu \delta\left(E_{\max} - E_e\right) + \frac{\alpha}{2\pi}\left[\left(\ln\frac{4E_{\max}^2}{m_e^2} - 2\right)\frac{E_e^2 + m_\mu^2}{m_\mu\left(E_{\max} - E_e\right)}\right]_+ + W\left(E_e\right), \quad (3)$$

where $E_{\max}$ is the conversion energy and $W\left(E_e\right)$ is the non-universal part of the correction. It depends on the electron energy E_e and details of the interaction that induces conversion. This part is not enhanced and can be neglected in the upcoming conversion searches. The definition of the "plus" distribution can be found in [27]. The correction to the spectrum is dominated by the collinear logarithm. The bound state logarithm of $Z\alpha$ modifies only the total conversion rate Γ_0. Formula (3) contains only the leading term in $Z\alpha$ expansion and, therefore, it predicts the spectrum with an accuracy of about 1% near the endpoint, much better than required by the upcoming experiments at Fermilab and J-PARC.

3.2. Decay of mesons

The QCD bound-states require a different approach than the QED bound-states. In the case of mesons, photons can be regarded as probes of the QCD structure of the confined quarks. Ultra-soft photons decouple from electrically neutral mesons, however, photons with wavelengths shorter than the size of the meson can resolve constituent quarks and probe their wave function. In the following section, we illustrate this mechanism on the example of recently computed power enhanced QED corrections for the leptonic decay of B_s meson [28].

A decay rate of a strange B meson into a pair of leptons is under exceptionally good theoretical control because the final state is purely leptonic. This means that the QCD interaction can be parametrized in terms of a decay constant alone at the leading order in QED because the QCD matrix element is local. Moreover, the decay is helicity suppressed in the Standard Model and, therefore, it is very sensitive to scalar currents generated by the beyond the SM physics.

Once the QED interactions are considered, the QCD matrix element cannot be parametrized in terms of the decay constant alone. Virtual and real photons can couple to quarks, hence a non-local time-ordered product of electromagnetic current and weak interaction Lagrangian have to be considered. Typically, these non-local matrix elements are hard to compute with the standard perturbative and non-perturbative methods, but in certain cases, the matrix element can be simplified due to a hierarchy of scales that allows employing EFT methods.

The appropriate EFT for the $B_s \to \mu^+\mu^-$ is heavy quark EFT combined with the soft-collinear EFT. It is obtained after decoupling of several scales: electroweak [29, 30] $\Lambda \sim m_W$, hard $\Lambda \sim m_b$ and hard-collinear $\Lambda \sim \sqrt{m_b \Lambda_{\mathrm{QCD}}}$. The dynamical degrees of freedom are soft-quark fields and collinear lepton fields. Soft photons are already decoupled from the collinear fields. The decay rate can then be computed as a systematic expansion in $\lambda = (\frac{\Lambda_{\mathrm{QCD}}}{m_b})^{\frac{1}{2}}$. For the counting purpose, we also take $m_\mu \sim \Lambda_{\mathrm{QCD}}$.

The expansion of the leading order partonic amplitude starts at $\mathcal{O}(\lambda^2)$ because of the helicity suppression factor. Interestingly, the expansion of the amplitude at the order of α starts at $\mathcal{O}(\lambda^0)$. The power enhancement of the correction is a result of "non-local annihilation". At the leading order in QED, the helicity flip and annihilation must occur at the same point, hence we refer to this situation as the "local annihilation". Beyond the leading order, this may not be the case. The annihilation and helicity flip may be separated by a light-like distance. The local hadronic matrix element $\langle 0|\, \bar{q}(0) \Gamma h_v(0)\, |\bar{B}_s(p)\rangle$ is replaced by a non-local matrix element

$$\langle 0|\, m_b \int \mathrm{d}x_- \bar{q}(x_-) \Gamma h_v(0)\, |\bar{B}_s(p)\rangle \tag{4}$$

that can be parametrized in terms of the light-cone distribution amplitude. The separation cannot be arbitrarily large, the meson size provides a natural infra-red cut-off $\sim \frac{1}{\Lambda_{\mathrm{QCD}}}$, hence the higher order amplitude is enhanced with respect to the tree-level by a factor $\frac{m_b}{\Lambda_{\mathrm{QCD}}}$.

The one-loop decay amplitude, shown in Fig. 2, can be computed using expansion by regions or by explicit computation. A SCET computation is particularly interesting as it reveals the origin of the correction. The starting

point is a $\mathrm{SCET_I}$ current [31] matched on the weak effective Lagrangian. The current may contain hard-collinear quark field, rather than a soft field and, therefore, it is enhanced with respect to the leading operator by two powers of λ. To obtain non-zero overlap with the B_s, the hard-collinear quark must be converted into a soft quark. A hard-collinear field scales like λ, while the soft field scales like λ^3 and for that reason, subleading $\mathrm{SCET_I}$ interactions must be used.

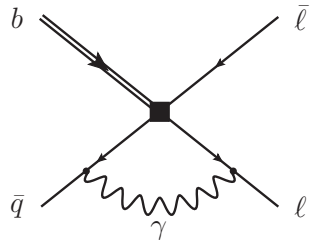

Fig. 2. A diagram contributing to the QED corrections to the decay rate of a strange meson, $B_s \to \mu^+\mu^-$. An exchange of a photon between the leptons and the light quark leads to the correction that is power enhanced with respect to the tree-level contribution.

In order to reproduce terms suppressed by the muon mass m_μ, we must consider subleading SCET collinear interactions of $\mathcal{O}(\lambda)$

$$\mathcal{L}_m^{(1)} = m_\mu \bar{\xi} \left[i \not{D}_\perp, \frac{1}{i n_+ D} \right] \frac{\not{n}_+}{2} \xi \,, \tag{5}$$

where ξ is collinear muon field. The light-cone coordinates are defined like in [31]. Remembering that interactions between soft and hard-collinear quarks start at the order of λ, we note that (5) gives the leading power contribution. The Lagrangian $\mathcal{L}_m^{(1)}$ contains muon field with opposite chirality as opposed to the leading power collinear interaction that does not flip chirality. Hence, terms obtained from $\mathcal{L}_m^{(1)}$ insertions do not require further helicity suppression. Terms obtained from the $\mathcal{O}(\lambda)$ interaction between soft and hard-collinear quarks and the leading power collinear interaction vanish by reparametrization invariance and so no further power-enhanced terms appear.

Explicit computation reveals additional logarithmic enhancements [28]. This changes the life-time by about 1%, exceeding the previous estimates [30]. Theoretical uncertainty of the $B_s \to \mu^+\mu^-$ decay rate is expected to be further reduced in a near future with a new QCD lattice computation of the B-meson decay constant and more precise determination of other parameters. This makes the evaluation of the QED correction important for the comparison of theory with the upcoming precise measurements.

4. Conclusions

Precise experiments searching for the new physics require a good theoretical understanding of the SM contribution. Recent computations of different corrections in bound states revealed unexpected enhancements and required to reexamine existing results. Upcoming experiments will require even more precise predictions, but systematic progress is possible thanks to modern EFT methods. Spectroscopic measurements allow to determine precisely fundamental constants and test the SM. Experiments operating at higher energies can directly probe potential new interactions in rare processes. In both cases, progress on the experimental side must by accompanied by better theoretical predictions. The QED corrections are an important ingredient of the precise SM computations, as shown by the examples invoked in this paper.

I thank Christoph Bobeth for useful comments and discussions. This work is supported by the DFG Sonderforschungsbereich/Transregio 110 "Symmetries and the Emergence of Structure in QCD".

REFERENCES

[1] A. Czarnecki, R. Szafron, *J. Univ. Sci. Tech. China* **46**, 407 (2016).

[2] H.A. Bethe, *Phys. Rev.* **72**, 339 (1947).

[3] P.J. Mohr, D.B. Newell, B.N. Taylor, *Rev. Mod. Phys.* **88**, 035009 (2016) [arXiv:1507.07956 [physics.atom-ph]].

[4] K. Pachucki, *Phys. Rev. A* **63**, 042503 (2001).

[5] U.D. Jentschura, A. Czarnecki, K. Pachucki, *Phys. Rev. A* **72**, 062102 (2005).

[6] A. Czarnecki, R. Szafron, *Phys. Rev. A* **94**, 060501 (2016) [arXiv:1611.04875 [physics.atom-ph]].

[7] C.G. Parthey *et al.*, *Phys. Rev. Lett.* **107**, 203001 (2011) [arXiv:1107.3101 [[physics.atom-ph]].

[8] S. Sturm *et al.*, *Nature* **506**, 467 (2014).

[9] J. Zatorski *et al.*, *Phys. Rev. A* **96**, 012502 (2017) [arXiv:1703.10649 [physics.atom-ph]].

[10] K. Pachucki, M. Puchalski, *Phys. Rev. A* **96**, 032503 (2017) [arXiv:1707.08518 [physics.atom-ph]].

[11] A. Czarnecki, M. Dowling, J. Piclum, R. Szafron, arXiv:1711.00190 [physics.atom-ph].

[12] V.A. Yerokhin, Z. Harman, *Phys. Rev. A* **95**, 060501 (2017) [arXiv:1704.08080 [physics.atom-ph]].

[13] V.A. Yerokhin *et al.*, *Phys. Rev. A* **94**, 022502 (2016) [arXiv:1606.08620 [physics.atom-ph]].

[14] G.F. Giudice, P. Paradisi, M. Passera, *J. High Energy Phys.* **1211**, 113 (2012) [arXiv:1208.6583 [hep-ph]].

[15] F. Jegerlehner, *EPJ Web Conf.* **118**, 01016 (2016) [arXiv:1511.04473 [hep-ph]].

[16] R. Szafron, F. Jegerlehner, *PoS* **RADCOR2011**, 035 (2011).

[17] F. Jegerlehner, R. Szafron, *Eur. Phys. J. C* **71**, 1632 (2011) [arXiv:1101.2872 [hep-ph]].

[18] K. Hagiwara *et al.*, *Nucl. Part. Phys. Proc.* **287–288**, 33 (2017).

[19] C.P. Burgess, P. Hayman, M. Rummel, L. Zalavari, arXiv:1708.09768 [hep-ph].

[20] C.P. Burgess, P. Hayman, M. Rummel, L. Zalavari, arXiv:1612.07337 [hep-ph].

[21] R. Szafron, *Acta Phys. Pol. B* **46**, 2279 (2015).

[22] R. Szafron, *Acta Phys. Pol. B* **44**, 2289 (2013).

[23] R. Szafron, A. Czarnecki, *Phys. Rev. D* **94**, 051301 (2016) [arXiv:1608.05447 [hep-ph]].

[24] A. Czarnecki *et al.*, *Phys. Rev. D* **90**, 093002 (2014) [arXiv:1406.3575 [hep-ph]].

[25] R. Szafron, A. Czarnecki, *Phys. Rev. D* **92**, 053004 (2015) [arXiv:1506.00975 [hep-ph]].

[26] R. Szafron, A. Czarnecki, *Phys. Lett. B* **753**, 61 (2016) [arXiv:1505.05237 [hep-ph]].

[27] R.D. Field, *Front. Phys.* **77**, 1 (1989).

[28] M. Beneke, C. Bobeth, R. Szafron, arXiv:1708.09152 [hep-ph].

[29] A.J. Buras, arXiv:hep-ph/9806471.

[30] C. Bobeth *et al.*, *Phys. Rev. Lett.* **112**, 101801 (2014) [arXiv:1311.0903 [hep-ph]].

[31] M. Beneke, T. Feldmann, *Nucl. Phys. B* **685**, 249 (2004) [arXiv:hep-ph/0311335].